Surface defect inspection of spherical objects by the resonant sphere technique

C. P. Hsieh and B. T. KhuriYakub

Citation: Appl. Phys. Lett. **60**, 1815 (1992); doi: 10.1063/1.107173
View online: http://dx.doi.org/10.1063/1.107173
View Table of Contents: http://apl.aip.org/resource/1/APPLAB/v60/i15
Published by the American Institute of Physics.

Surface defect inspection of spherical objects by the resonant sphere technique

C. P. Hsieh and B. T. Khuri-Yakub
Edward L. Ginzton Laboratory, Stanford University, Stanford, California 94305-4085

(Received 19 December 1991; accepted for publication 7 February 1992)

Ceramic materials, such as silicon nitride and silicon carbide, are important because of their high mechanical strength at high temperature and in nonlubricative environments. The weakness of these materials lies in their brittleness. Stress concentration caused by the existence of surface or subsurface cracks can lead to the total mechanical failure of parts. In this letter, we describe the application of the resonant-sphere technique to perform nondestructive evaluation of ceramic bearing balls. The technique had been shown to be capable of measuring various material properties, such as V_s (shear wave velocity) and ν (Poisson's ratio). We use phase and amplitude measurements to simplify the evaluation of various resonance quality factors (Q), and we present, for the first time, the use of a resonance technique to propagate and detect surface waves on a sphere. We also show a decrease in Q for surface-wave modes due to the existence of surface cracks.

The resonant-sphere technique[1] was introduced by Fraser in 1964 as a tool for material property measurement.[2] Considering the characteristic equation of a resonant sphere, one can theoretically calculate the relationship between the resonant frequencies and the material properties, such as V_s and ν. By using the resonant frequency of the first several fundamental modes, the mechanical properties can be calculated. The notations we use are S_{mn} for the nth mode for the mth harmonic of the spheroidal resonances and T_{pq} for the qth mode for the pth harmonic of the torsional resonances. The special cases here are the S_{0n} modes, which are pure longitudinal modes. Also, the S_{m0} modes for m large had been shown to be the resonance modes for surface acoustic waves (Rayleigh waves).[3]

The experimental setup is shown in Fig. 1. A signal from the first synthesizer is sent to the bottom $LiNbO_3$ longitudinal transducer, which excites ultrasonic waves on the sphere, in this case, a ceramic bearing ball. The top transducer, which is similar to the bottom transducer, acts as a receiver. It is positioned to make a Hertzian contact with the sphere. The received signal is mixed with a signal from the second synthesizer with a frequency setting which is 1 kHz lower than that of the first synthesizer. After mixing, the signal is sent into a lock-in amplifier where its amplitude and phase are measured. Signals from the trigger output channels of both synthesizers are also mixed, low-pass filtered at 1 kHz, and then sent into the reference channel of the lock-in amplifier. We designed a computer-controlled system to sweep over the frequency range of interest and were thus able to measure the resonant frequency spectrum of the spheres. Local maxima in amplitude are used to determine the resonance frequencies of the sphere, whereas the phase of the spectrum is used to measure the resonance Q's.

Using amplitude alone to measure samples with high Q's is time consuming because of the small frequency increment necessary for an accurate measurement. The importance of phase measurement is evident for this reason. At resonance, phase undergoes a change of π and its slope $d(\text{phase})/d(\text{frequency})$ is almost constant. The equation for phase near resonance is given by[4]

$$\theta = \theta_0 - \tan^{-1}\frac{(f^2 - f_0^2)Q}{f f_0},$$

where θ_0 is the phase value at resonance, f_0 is the resonance frequency, f is the frequency at each point, and Q is the quality factor. Therefore, to determine the resonance Q for a particular mode, we simply determine the resonant frequency to the desired accuracy, measure several points around resonance, and fit a curve to the measured phase according to the above equation.

Three Si_3N_4 ceramic bearing balls of 1/2 in. diameter were used as samples for the experiment. The first ball is perfect with no cracks. The second had a series of cracks made with a 10 g load on an indenter, and the third had

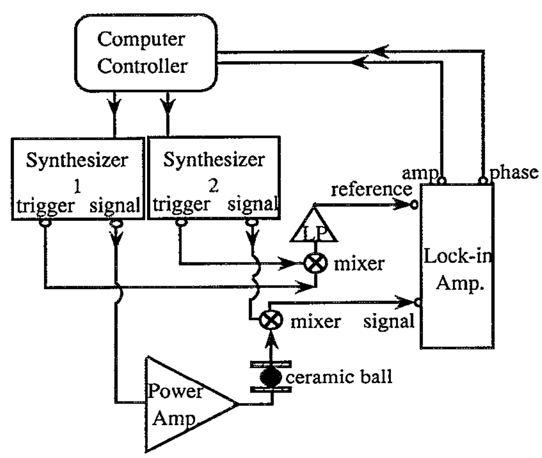

FIG. 1. Experimental setup for the resonant-sphere technique.

 0003-6951/92/151815-03$03.00

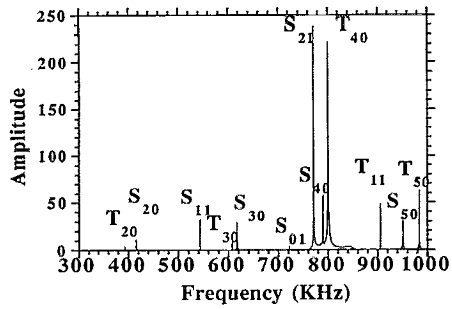

FIG. 2. Spectrum in amplitude for the fundamental modes of ball C.

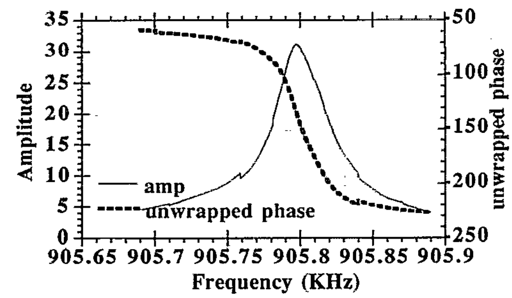

FIG. 3. Spectrum in both amplitude and phase for mode T_{12} of ball A. Curve fitting the phase information gives $Q = 34\,799$. One can see clearly the phase change near resonance.

cracks made with a load of 50 g on the indenter (for simplicity, we will hereafter refer to these three balls as A, B, and C). Our motivation is to determine the effect of surface imperfections on the resonance Q's of surface-wave modes because surface cracks will scatter surface waves. Thus, by properly rotating the samples, the existence of surface cracks should lower the surface-wave resonance Q's.

First, we determine the mechanical properties of the samples. Figure 2 shows an example of the amplitude-frequency spectrum of ball C. Figure 3, in turn, zooms in on the amplitude and phase of a particular high-Q mode T_{12} of ball A. Among the numerous torsional modes of a sphere, the T_{p2} modes showed the highest Q value. This may be due to the fact that the displacement amplitude of the T_{p2} modes are large mainly inside the sphere.[2] High-Q modes are more frequency selective and are chosen to calculate the mechanical properties. Table I lists the material constants calculated from the resonant frequencies for the three samples. V_s was calculated from the T_{12} mode and ν was determined from the T_{12} and S_{01} modes by solving the characteristic equations. V_l was calculated from V_s and ν. V_R is calculated from the characteristic equation for surface waves.[3]

When the frequency of interest gets higher, the resonance spectrum becomes more complicated as there is an increasing number of closely spaced higher-order resonance modes. Still, it was possible to isolate the surface-wave resonances, as shown in Fig. 4. Several dominating resonance modes which are almost equally spaced in the frequency domain are in evidence.

Several reasons lead us to conclude that these dominating modes are indeed surface-wave resonance modes. First, surface waves on a sphere tend to dominant in the higher frequency region. Second, when combining the asymptotic characteristic equation of surface waves on a sphere with material properties acquired in the low-frequency region, we calculate the surface-wave velocity V_R and the corresponding wavelength $\lambda_R = V_R(\text{calculated})/f(\text{measured})$. We then ascertain that an integer number of half wavelength fits on the surface of the sphere according to the relationship $\pi r/(\lambda_R/2) = n$, where n is a large positive integer, around 50 in our case. Third, for the same sphere, the values of the resonance Q's for the dominating modes are of similar values; this indicates that these modes are of similar character. We therefore conclude that these dominating modes are surface-wave modes.

TABLE I. Data obtained by the resonant-sphere technique for three ceramic bearing balls, each with a diameter of 1/2 in. Ball A is a perfect ball with no cracks. Ball B had a series of cracks made with a 10 g load on a Knoop indenter, and ball C had the cracks with a load of 50 g on the Knoop indenter. V_R is the surface-wave velocity, and $\lambda_R = V_R/f$ is the wavelength of the surface wave at frequency f.

	Ball A	Ball B	Ball C
f_{T12} (KHz)	905.80	905.74	905.50
Q_{T12}	34 799	42 242	32 985
f_{S01} (KHz)	720.41	724.42	721.40
Q_{S01}	20 058	19 245	16 918
V_s(m/s)	6270.5	6270.1	6268.4
ν	0.26447	0.26573	0.26522
V_l(m/s)	11 081	11 100	11 082
V_R(m/s)	5779.9	5780.8	5778.8

Results for surface waves

$\pi r/\lambda_R$	f(MHz)	Q	f(MHz)	Q	f(MHz)	Q
49.0	14.1963	10 810	14.2090	7905	14.1790	3655
49.5	14.3409	11 321	14.3547	7998	14.3252	4348
50.0	14.4855	9 573	14.4988	8546	14.4677	4607

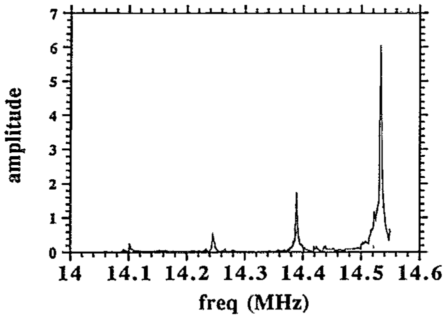

FIG. 4. Spectrum in amplitude for ball A around 14.25 MHz. The dominance of surface waves is evident.

Table I also shows the results of measurements of the three balls for three surface-wave resonance modes. We note that the Q of the surface-wave resonances decrease as the load on the indenter, and consequently, the sizes of the surface cracks increase. Thus, we have a direct relationship between the value of the Q of the surface-wave resonance and the density of surface defects.

In conclusion, we have successfully used the resonant-sphere technique with an improved amplitude- and phase-measurement system to identify low-frequency resonances from which we acquire material properties. We also demonstrated, for the first time, that this technique can be applied in the higher-frequency region to identify surface waves on a sphere, and we related the quality factor of surface-wave resonances to the density of surface defects.

This work was supported by the Department of Energy under Contract No. DE-FGO3-84ER45157.

[1] D. B. Fraser and R. C. LeCraw, Rev. Sci. Instrum. **35**, 1113 (1964).
[2] Naohiro Soga and Orson L. Anderson, J. Geophys. Res. **72**, 1733 (1967).
[3] Yasuo Satô and Tatsuo Usami, Geophys. Mag. **31**, 25 (1962).
[4] James W. Nilsson, in *Electric Circuits* (Addison-Wesley, Reading, MA, 1986), pp. 514–518.